

# Relaxation times of unstable states in systems with long range interactions

Kavita Jain<sup>1</sup>, Freddy Bouchet<sup>2</sup> and David Mukamel<sup>1</sup>

<sup>1</sup> Department of Physics of Complex Systems, The Weizmann Institute of Science, Rehovot 76100, Israel

<sup>2</sup> Institut Non Linéaire de Nice (INLN), CNRS, UNSA UMR 6618, 1361 Route des Lucioles, F-06560 Valbonne, France

E-mail: [jain@jncasr.ac.in](mailto:jain@jncasr.ac.in), [Freddy.Bouchet@inln.cnrs.fr](mailto:Freddy.Bouchet@inln.cnrs.fr) and [david.mukamel@weizmann.ac.il](mailto:david.mukamel@weizmann.ac.il)

Received 10 September 2007

Accepted 23 October 2007

Published 19 November 2007

Online at [stacks.iop.org/JSTAT/2007/P11008](http://stacks.iop.org/JSTAT/2007/P11008)

doi:10.1088/1742-5468/2007/11/P11008

**Abstract.** We consider several models with long range interactions evolving via Hamiltonian dynamics. The microcanonical dynamics of the basic Hamiltonian mean field (HMF) model and perturbed HMF models with either global anisotropy or an on-site potential are studied both analytically and numerically. We find that, in the magnetic phase, the initial zero magnetization state remains stable above a critical energy and is unstable below it. In the dynamically stable state, these models exhibit relaxation timescales that increase algebraically with the number  $N$  of particles, indicating the robustness of the quasistationary state seen in previous studies. In the unstable state, the corresponding timescale increases logarithmically in  $N$ .

**Keywords:** classical phase transitions (theory), phase diagrams (theory)

---

**Contents**

<b>1. Introduction</b>	<b>2</b>
<b>2. Isotropic Hamiltonian mean field model</b>	<b>4</b>
<b>3. Anisotropic Hamiltonian mean field model</b>	<b>8</b>
<b>4. Hamiltonian mean field model with on-site potential</b>	<b>11</b>
<b>5. How long is the Vlasov approximation valid?</b>	<b>15</b>
<b>6. Conclusions</b>	<b>16</b>
<b>Acknowledgments</b>	<b>17</b>
<b>References</b>	<b>17</b>

---

**1. Introduction**

In recent years, much work has been devoted to the understanding of the statistical mechanics and the dynamics of systems with long range interactions. In these systems the interaction potential between two particles decays at large distances  $r \gg 1$  as  $V(r) \sim r^{-\alpha}$  with  $\alpha \leq d$ ,  $d$  being the dimension of the system. Examples of such systems include self-gravitating systems, two-dimensional and geophysical vortices, non-neutral plasma, and systems describing wave-particle interactions (free-electron laser, CARL experiment, etc) and magnetic dipolar systems (see [1] for reviews).

The long range nature of the interactions makes these systems non-additive. Due to this property, at statistical equilibrium, inequivalence between the microcanonical and the canonical ensembles is a generic feature. This was first observed in models of self-gravitating stars [2, 3], and then seen in a number of other models ranging from the point vortex model [4, 5], plasma physics [6], self-gravitating systems [7, 8], two-dimensional flows [9] and long range Hamiltonian models [10, 11] to simple spin models with mean field interactions [12, 13]. A classification of phase transitions and ensemble inequivalence in generic long range systems [14] has shown that many possible types of behavior remain to be seen in specific physical systems.

Beside these equilibrium peculiarities, the dynamics of systems with long range interactions also present several new features. For a large number  $N$  of particles, these systems may exhibit quasi-stationary states (QSS) [15, 16] (in the plasma or astrophysical context, see for instance [17, 18]), very long relaxation time [16], vanishing Lyapounov exponents [15, 19], anomalous relaxation and diffusion [20]–[24] and breaking of ergodicity [13, 25]. These features are a result of similar collective (self-consistent) dynamics [26] shared by systems with long range interactions. In the limit of a large number of particles, such dynamics is well approximated by kinetic theories [18, 23], [27]–[29] which to leading order in  $1/\sqrt{N}$  describe Vlasov type dynamics, and after much longer time, the relaxation towards equilibrium is governed by Lennard-Balescu type dynamics.

In this paper, we consider the dynamics of systems with long range interactions and analyze the time it takes for a system to relax to its equilibrium state, starting from

a thermodynamically unstable state. The relaxation process is usually initiated by the formation of droplets of the equilibrium state which is followed by a coarsening process [30]. In systems with short range interactions, the initial droplets are of a typical radius which does not grow with the system size. As a result, the characteristic time for the formation of such droplets is also independent of the system size. On the other hand, in systems with long range interactions the relaxation timescale diverges with the system size  $N$ . This may result in long lived, quasistationary states (QSS) which are not the true equilibrium state of the system but which relaxes to the equilibrium state on timescales that increase algebraically with  $N$ .

Such long-lived states have been seen, for instance, in numerical studies of long-ranged spin models [16]. These QSS have been explained as stable stationary states of the Vlasov equation and may lead to anomalous diffusion [23, 31]. We note that an alternative explanation, both for the existence of QSS and for anomalous diffusion, has been proposed in the context of Tsallis non-extensive statistical mechanics [32, 33] (see [16] and [23] for further discussions). Recent studies have considered the possible prediction of QSS using the equilibrium statistical mechanics of the Vlasov equation [34]–[36]. The issue of the robustness of QSS when the Hamiltonian is perturbed by short range interactions [37] or when the system is coupled to an external bath [38, 39] has also been addressed, and it was found that, while the power law behavior survives, the exponent may not be universal. Such a slow relaxation is not the only possible behavior in these systems<sup>3</sup>. A recent consideration of the thermodynamic stability of a mean field Ising model with stochastic dynamics has found the relaxation time to be logarithmic in  $N$  [13]. It is thus of interest to study the slow relaxation processes in systems with long range interactions and explore in more detail the possible resulting timescales involved.

With this aim in mind, we consider the microcanonical dynamics of a generalized Hamiltonian mean field (HMF) model which is a simple prototype of long-ranged systems by adding a global anisotropy term or an on-site potential energy term to the Hamiltonian. The basic HMF model ([40], see also [41]–[45]) describes a system of  $N$  classical  $XY$  rotors with mean field coupling. Adding new terms to the Hamiltonian allows one to vary an external parameter (such as anisotropy) and explore a richer phase diagram. Our analysis of the Vlasov equation for these models shows that both logarithmic and power law behavior are generically present in long-ranged systems. It is found that at low energies the non-magnetic solution is dynamically unstable and the system relaxes to the magnetically ordered state on a logarithmic timescale which follows from the dynamic instability of the Vlasov equation. At higher energies, but still within the magnetic state, the non-magnetic solution becomes linearly stable (although it is not the true equilibrium state of the system) and the relaxation takes place on algebraically diverging timescales and QSS are observed. We show the existence of QSS using analytic relations for the marginal stability of the Vlasov equation. These results give further insight into the robustness of QSS states when the interaction potential is perturbed.

Most of the QSS studied so far have dealt with homogeneous situations (namely states whose distribution functions do not depend on the angle or spatial variable). From a theoretical point of view, inhomogeneous QSS should exist in the same way as homogeneous ones. The main reason why such states have not been studied in detail is

<sup>3</sup> Relaxation times can be exponentially long if the initial state is metastable which we do not consider here.

the difficulty to deal theoretically with the inhomogeneous marginal stability equation. The QSS of the HMF model with on-site potential described in section 4 is an example of inhomogeneous QSS. Moreover, the new method we propose to study them can be applied to other situations, and also, for instance, to the usual isotropic HMF model.

The relaxation times mentioned above are interesting from another viewpoint. Since the rationale for the existence of QSS is based on the approximation of the  $N$  particle dynamics by a Vlasov dynamics, a crucial issue is the understanding of the validity of such an approximation. In a classical work by Braun and Hepp [46], it was proved that this approximation is valid for time  $t$  smaller than  $t_V(N)$  for smooth interaction potential and large enough  $N$ . Following the reasoning of [46] allows one to conclude that a lower bound for  $t_V(N)$  is proportional to  $\ln N$  for large  $N$ . A recent paper [47] showed that, for initial conditions close to some homogeneous QSS, a lower bound for  $t_V(N)$  scales like  $N^{1/8}$ . In section 5, we give two new results concerning this issue. First, we prove that the Braun and Hepp result is actually optimal. More precisely, we show that, for some initial conditions, the kinetic description is not valid for time larger than  $\sim \ln N$ . Second, we argue that most of the trajectories will have  $t_V$  either equal to the lifetime of a QSS (possibly algebraic), or logarithmically long  $t_V$ , depending on the way the relaxation towards equilibrium takes place.

The rest of this paper is organized as follows. In section 2, we define the HMF model and study its dynamically unstable state in detail using the Vlasov equation and numerical simulations. The anisotropic HMF model is the subject of section 3 in which the dynamical phase diagram is obtained analytically in the energy-anisotropy plane. The model with on-site potential is introduced and discussed in section 4. The issue of the timescale over which the Vlasov equation holds is discussed in section 5. Finally, we conclude with a summary and open questions in section 6.

## 2. Isotropic Hamiltonian mean field model

In this section, we consider the dynamics of the Hamiltonian mean field (HMF) model which is defined by the Hamiltonian

$$H = \sum_{i=1}^N \frac{p_i^2}{2} + \frac{1}{2N} \sum_{i,j=1}^N [1 - \cos(\theta_i - \theta_j)], \quad (1)$$

where  $\theta_i$  and  $p_i$  are the phase and momentum of the  $i$ th particle, respectively, and  $N$  is the number of particles. In the equilibrium state, a second-order phase transition between the ferromagnetic and paramagnetic state occurs at the critical energy density  $\epsilon_c = 3/4$ . This has been shown in the canonical ensemble [40] and later verified for the microcanonical ensemble using the large deviations' method [48].

The time evolution of this system starting far from the equilibrium state has been studied using Hamiltonian dynamics. The angle  $\theta_i$  and momentum  $p_i$  of the  $i$ th particle obey

$$\frac{d\theta_i}{dt} = p_i \quad (2)$$

$$\frac{dp_i}{dt} = -m_x \sin \theta_i + m_y \cos \theta_i, \quad (3)$$

where  $m_x$  and  $m_y$  are the components of the magnetization density

$$\vec{m} = \left( \frac{1}{N} \sum_{i=1}^N \cos \theta_i, \frac{1}{N} \sum_{i=1}^N \sin \theta_i \right). \quad (4)$$

The dynamics conserves the total energy and the total momentum. We start with an initial condition with randomly distributed  $\theta_i \in [-\pi, \pi]$  so that the average magnetization is zero and the standard deviation about the mean is of the order of  $\sim 1/\sqrt{N}$ . To fix the total energy density  $\epsilon$ , the momentum is chosen from a distribution  $f^{(0)}(p)$  with  $p_i$  lying in the interval  $[p_{\min}, p_{\max}]$ . In this paper, we consider the following choices of momentum distribution

$$f^{(0)}(p) = \begin{cases} (1/2p_0), & p \in [-p_0, p_0] \\ \sqrt{\beta/2\pi} \exp(-\beta p^2/2), & p \in (-\infty, \infty) \end{cases} \quad (5)$$

where the parameter  $p_0$  in the uniform (or waterbag) distribution and  $\beta$  in the Gaussian case are related to the energy as

$$\begin{aligned} p_0 &= \sqrt{6\epsilon - 3}, \\ \beta &= 1/(2\epsilon - 1). \end{aligned} \quad (6)$$

The equations of motion (2) and (3) are integrated using a symplectic fourth-order integrator with time step  $dt = 0.1$ . The reference coordinate axes in which  $\theta_i$  is measured is specified by the initial magnetization.

To study the dynamical behavior of magnetization, we first recall the classical computation of the Vlasov equation [27, 46], [49]–[51] (see also [40] for the HMF model). The probability density  $f_d(\theta, p, t)$  which counts the number of particles with angle  $\theta$  and momentum  $p$  at time  $t$  can be written as

$$f_d(\theta, p, t) = \frac{1}{N} \sum_{i=1}^N \delta(\theta_i(t) - \theta) \delta(p_i(t) - p). \quad (7)$$

Taking the time derivative of both sides of the above equation and using the canonical equations of motion, one obtains

$$\frac{\partial f_d}{\partial t} + p \frac{\partial f_d}{\partial \theta} - \frac{\partial V}{\partial \theta} \frac{\partial f_d}{\partial p} = 0, \quad (8)$$

where the average potential  $V(\theta, t)$  is given by

$$V(\theta, t) = \int_{p_{\min}}^{p_{\max}} dp' \int_{-\pi}^{\pi} d\theta' (1 - \cos(\theta - \theta')) f_d(\theta', p', t). \quad (9)$$

Expanding (7) to leading orders in  $1/\sqrt{N}$  (see below), we obtain the Vlasov equation obeyed by the (smooth) distribution  $f(\theta, p, t)$  for infinite  $N$ :

$$\frac{\partial f}{\partial t} + p \frac{\partial f}{\partial \theta} - \frac{\partial V}{\partial \theta} \frac{\partial f}{\partial p} = 0. \quad (10)$$

It is easily verified that the initial condition with angles distributed uniformly and momentum chosen from an arbitrary (normalized) distribution  $f^{(0)}(p)$  is, in fact, a

stationary state of this equation. To deal with the finite  $N$  case, we treat the finiteness as a perturbation about the homogeneous stationary state of the infinite system:

$$f(\theta, p, t) = \frac{1}{2\pi} f^{(0)}(p) + \lambda f^{(1)}(\theta, p, t), \quad (11)$$

where, after linearization, the perturbed distribution  $f^{(1)}$  is a solution of the integro-differential equation

$$\frac{\partial f^{(1)}}{\partial t} + p \frac{\partial f^{(1)}}{\partial \theta} - \frac{1}{2\pi} \frac{\partial f^{(0)}}{\partial p} \int dp' d\theta' f^{(1)}(\theta', p', t) \sin(\theta - \theta') = 0. \quad (12)$$

Since the initial angles and momentum of the  $N$  particles are sampled according to the distribution  $f^{(0)}$ , the small parameter  $\lambda$  is of the order of  $1/\sqrt{N}$ .

We now study the linear dynamics about the distribution  $f^{(0)}(p)/2\pi$  by considering the eigenmodes of (12). A first treatment of the linear stability of stationary solutions of the HMF equation can be found in [45] (see also [26] and [16]). As is explained, for instance, in textbooks on plasma physics [27], any arbitrary function  $f^{(1)}(\theta, p, t)$  cannot be decomposed into the eigenmodes of the linearized equation (12). However, when unstable modes exist, after a short time the largest of them dominates the dynamics and therefore at sufficiently long times, the temporal behavior can be described by the eigenmodes. We define the Fourier modes  $f_k^{(1)}(p, \omega)$  (and the conjugate  $f_{-k}^{(1)}$ ) as the eigenmodes of (12) of type

$$f^{(1)}(\theta, p, t) = f_k^{(1)}(p, \omega) e^{i(k\theta + \omega t)}. \quad (13)$$

Since the last term in the Vlasov equation (12) involves only  $e^{\pm i\theta}$ , the Fourier modes must have  $k = \pm 1$ . The coefficients  $f_{\pm 1}^{(1)}$  are then determined by

$$f_{\pm 1}^{(1)}(p, \omega) + \frac{1}{2} \frac{\partial f^{(0)}}{\partial p} \frac{\int_{p_{\min}}^{p_{\max}} dp' f_{\pm 1}^{(1)}(p', \omega)}{p \pm \omega} = 0. \quad (14)$$

Integrating over  $p$  on both sides, one gets

$$I_{\pm}(1 - J_{\pm}) = 0 \quad (15)$$

where

$$I_{\pm} = \int_{p_{\min}}^{p_{\max}} dp f_{\pm 1}^{(1)}(p), \quad J_{\pm} = -\frac{1}{2} \int_{p_{\min}}^{p_{\max}} \frac{dp}{p \pm \omega} \frac{\partial f^{(0)}}{\partial p}. \quad (16)$$

The frequency  $\omega$  is thus found from the condition  $J_{\pm} = 1$ . For initial distributions  $f^{(0)}$  which are even for the variable  $p$ , this condition yields an equation in  $\omega^2$ . We now consider specific choices of momentum distribution  $f^{(0)}(p)$ . For uniformly distributed initial momentum, the frequency determined using the condition  $J_{\pm} = 1$  works out to be [40]

$$\omega^2 = 6 \left( \epsilon - \frac{7}{12} \right). \quad (17)$$

For  $\epsilon > \epsilon^* = 7/12$ , unstable modes do not exist and the Vlasov equation is linearly stable. It is, however, unstable for  $\epsilon < \epsilon^*$  and the perturbation  $f^{(1)}(\theta, p, t)$  grows exponentially fast towards the equilibrium state. Setting  $\omega^2 = -\Omega^2$  for  $\Omega$  real, we have

$$f^{(1)}(\theta, p, t) = A f_1^{(1)}(\theta, p) e^{\Omega t} \quad (18)$$

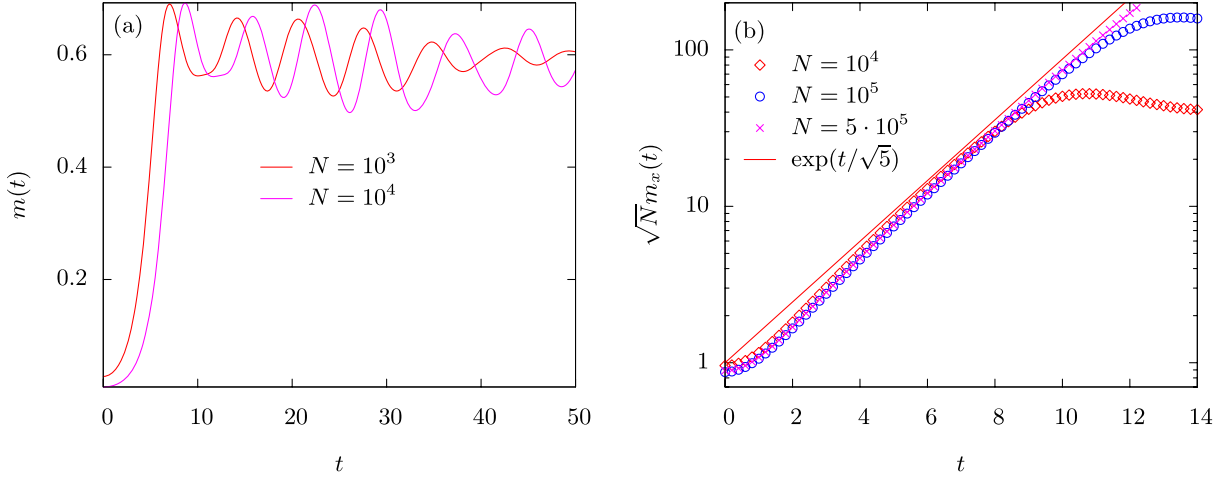


**Figure 1.** (a) Time evolution of the average magnetization  $m(t)$  in the unstable phase at  $\epsilon = 0.55$  for two values of  $N$ . (b) Data collapse for the scaled magnetization  $\sqrt{N}m_x(t)$  versus  $t$  on the semi-logarithmic scale. The slope  $\Omega = 1/\sqrt{5}$  of the solid line is given by (17). The data have been averaged over 200 histories for each  $N$ .

where  $A$  is a constant. As mentioned above, this time dependence is valid for times  $t \gg 1/\Omega$ . To treat the behavior at short times, the finite  $N$  behavior in the initial condition must be taken into account [27].

The average magnetization along the  $x$  and  $y$  axes, which are the observables of interest, can be written as

$$(m_x(t), m_y(t)) = \int_{p_{\min}}^{p_{\max}} dp \int_{-\pi}^{\pi} d\theta (\cos \theta, \sin \theta) f(\theta, p, t) \quad (19)$$

$$= \lambda \int_{p_{\min}}^{p_{\max}} dp \int_{-\pi}^{\pi} d\theta (\cos \theta, \sin \theta) f^{(1)}(\theta, p, t) + \mathcal{O}(\lambda^2). \quad (20)$$

The magnitude of the average magnetization is given by  $m = \sqrt{m_x^2 + m_y^2}$  and grows as

$$m \sim \frac{1}{\sqrt{N}} e^{\Omega t}. \quad (21)$$

The results of our simulations in figure 1(a) show that, after a transient, the magnetization grows exponentially, as expected on the basis of the preceding equation. Since the order of magnitude of the constant  $A$  in (18) is proportional to  $1/\sqrt{N}$ , the scaled magnetization  $\sqrt{N}m_x$  in figure 1(b) collapses into a single curve. The growth rate is also in agreement with  $\Omega$  obtained in (17). The above perturbative analysis cannot hold at long times as the linearization of the Vlasov equation breaks down when the magnetization reaches a value of order one. A similar analysis can be carried out for the Gaussian distributed initial momentum. In this case, we obtain that the modes exist only for  $\epsilon < \epsilon^* = 3/4$  and the eigenvalues of the modes are given by (37) with  $D = 0$ . Thus, (21) is obeyed in this case as well with the corresponding eigenfrequency. From (21), we see that the timescale on which the system acquires a finite  $m$  diverges as  $\ln N$ . Although this is the

same behavior as in the thermodynamically unstable phase of Ising model [13], the origin of the logarithmic timescale here is dynamical while it follows from an argument based on thermodynamics in the Ising case.

So far we have discussed the dynamical instability. The above argument gives a  $\ln N$  timescale for relaxation for  $\epsilon < \epsilon^*$ . Statistical mechanics predicts that homogeneous states are thermodynamically unstable for all (allowed) values of  $\epsilon < \epsilon_c = 3/4$ . For  $\epsilon^* < \epsilon < \epsilon_c$ , the distribution  $f^{(0)}(p)$  is dynamically stable but thermodynamically unstable. The relaxation is then not due to a dynamical instability and one then observes a  $N^{1.7}$  timescale (see [16]).

### 3. Anisotropic Hamiltonian mean field model

In this section, we consider the dynamics of the anisotropic HMF model defined by the Hamiltonian

$$H = \sum_{i=1}^N \frac{p_i^2}{2} + \frac{1}{2N} \sum_{i,j=1}^N [1 - \cos(\theta_i - \theta_j)] - \frac{D}{2N} \left[ \sum_{i=1}^N \cos \theta_i \right]^2, \quad (22)$$

where the last term represents the energy due to a global anisotropy in the magnetization along the  $x$  axis. At zero temperature, if  $D$  is positive, the equilibrium magnetization is along the  $x$  axis. Similarly for  $D < 0$ , the internal energy is lowered when the magnetization is along the  $y$  direction. For simplicity we consider below the case  $D > 0$ . To study the equilibrium phase diagram, consider the partition function in the canonical ensemble:

$$Z = \int \prod_{i=1}^N dp_i d\theta_i e^{-\beta H} = \left( \frac{2\pi e^{-\beta}}{\beta} \right)^{N/2} \int \prod_i d\theta_i \exp \left[ \frac{\beta N}{2} ((1+D)m_x^2 + m_y^2) \right]. \quad (23)$$

On using a Hubbard–Stratonovich transformation [40], the integrals over angles can be rewritten as

$$Z_\theta = \frac{N}{2\pi\beta\sqrt{(1+D)}} \int db_x db_y \exp \left[ -N \left( \frac{b_y^2}{2\beta} + \frac{b_x^2}{2\beta(1+D)} - \ln \int_{-\pi}^{\pi} d\theta e^{b_x \cos \theta + b_y \sin \theta} \right) \right], \quad (24)$$

where the double integral can be evaluated using the saddle point method for large  $N$ , leading to the free energy per particle

$$f = \frac{-\ln Z}{N\beta} = \frac{-1}{2\beta} \ln \left( \frac{2\pi}{\beta} \right) + \frac{1}{\beta} \left[ \frac{\bar{b}_x^2}{2\beta(1+D)} + \frac{\bar{b}_y^2}{2\beta} - \ln \int_{-\pi}^{\pi} d\theta e^{\bar{b}_x \cos \theta + \bar{b}_y \sin \theta} \right]. \quad (25)$$

In the above expression,  $\bar{b}_x$  and  $\bar{b}_y$  are determined by maximizing  $Z_\theta$  with respect to  $b_x$  and  $b_y$ , and are related to the equilibrium magnetization  $\bar{m}_x$  and  $\bar{m}_y$  along the  $x$  and  $y$  axis, respectively, as  $\bar{b}_x = \beta(1+D)\bar{m}_x$  and  $\bar{b}_y = \beta\bar{m}_y$ . As explained above, for  $D > 0$ , the system orders along the  $x$  axis and the magnetization  $\bar{m}_x$  is determined by

$$\bar{m}_x = \frac{\int_{-\pi}^{\pi} d\theta \cos \theta e^{\beta(1+D)\bar{m}_x \cos \theta}}{\int_{-\pi}^{\pi} d\theta e^{\beta(1+D)\bar{m}_x \cos \theta}}. \quad (26)$$

Close to the critical point, the above transcendental equation can be expanded in a Taylor series about zero magnetization and we obtain  $\overline{m}_x^2 = (8\beta(1+D)-16)/((4-\beta(1+D))\beta^2(1+D)^2)$  for  $D > 0$ . The inverse critical temperature at which magnetization vanishes is given by  $\beta_c = 2/(1+D)$ . The critical energy  $\epsilon_c$  can be calculated using the free energy expression above and we obtain

$$\epsilon_c = \left[ \frac{\partial(\beta f)}{\partial\beta} \right]_{\beta=\beta_c} = \frac{3+D}{4}. \quad (27)$$

For the anisotropic Hamiltonian, the equations of motion are similar to those for the isotropic case, (2) and (3), except that  $m_x$  is replaced by  $(1+D)m_x$ . The average potential appearing in the corresponding Vlasov equation (10) is now given by

$$V(\theta, t) = \int_{p_{\min}}^{p_{\max}} dp' \int_{-\pi}^{\pi} d\theta' [1 - \cos(\theta - \theta') - D \cos\theta \cos\theta'] f(\theta', p', t). \quad (28)$$

It can be checked that the homogeneous state (in  $\theta$ ) is a stationary state of the Vlasov equation for the anisotropic HMF model so that the distribution  $f(\theta, p, t)$  can be written as (11). The distribution  $f^{(1)}$  is now a solution of the following equation:

$$\frac{\partial f^{(1)}}{\partial t} + p \frac{\partial f^{(1)}}{\partial \theta} - \frac{1}{2\pi} \frac{\partial f^{(0)}}{\partial p} \int dp' d\theta' f^{(1)}(\theta', p', t) [\sin(\theta - \theta') + D \sin\theta \cos\theta'] = 0. \quad (29)$$

As before, going to the Fourier space and picking the coefficient of  $e^{\pm i\theta}$ , we obtain

$$I_{\pm} = \left[ \left(1 + \frac{D}{2}\right) I_{\pm} + \frac{D}{2} I_{\mp} \right] J_{\pm} \quad (30)$$

where  $I_{\pm}$  and  $J_{\pm}$  are given in (16). For  $D \neq 0$ , the frequency  $\omega$  is then determined through

$$(1+D)J_+J_- - \left(1 + \frac{D}{2}\right)(J_+ + J_-) + 1 = 0 \quad (31)$$

which is a *bilinear* equation unlike in the isotropic case. We now find the dynamical phase diagram and the frequency in the unstable phase for two choices of initial momentum distribution.

*Uniform distribution.* For uniformly distributed  $f^{(0)}(p)$ , the integrals  $J_{\pm}$  appearing in (31) can be readily done and we obtain a fourth-order equation for the frequency  $\omega$ :

$$4(\omega^2 - p_0^2)^2 + 2(2+D)(\omega^2 - p_0^2) + (1+D) = 0 \quad (32)$$

with the following four solutions:

$$\omega^2 = 6 \left( \epsilon - \frac{7+D}{12} \right) \quad (33)$$

$$\omega'^2 = 6 \left( \epsilon - \frac{7}{12} \right). \quad (34)$$

The frequency  $\omega^2$  vanishes at  $\epsilon^* = (7+D)/12$  while  $\omega'^2$  becomes zero at  $\epsilon'^* = 7/12$ . Thus in the magnetically ordered phase,  $\epsilon < \epsilon_c$ , three regions can be identified: a linearly

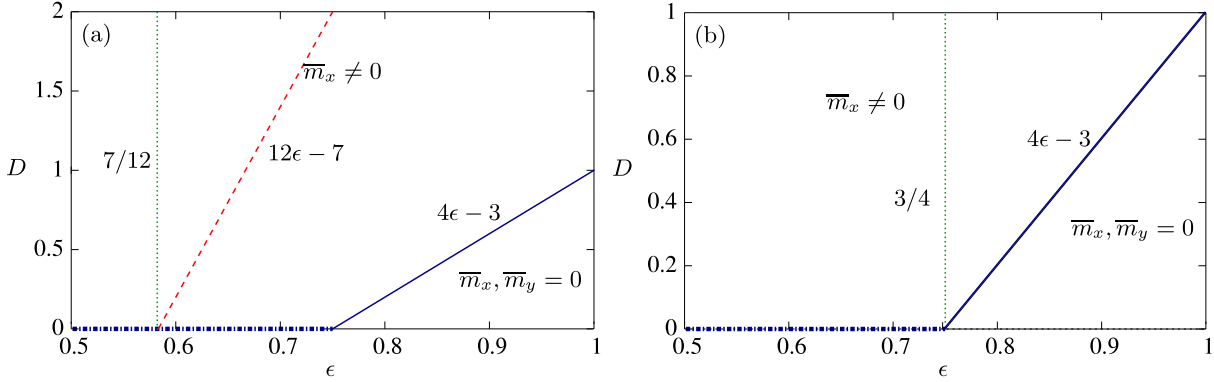


**Figure 2.** Dynamical phase diagram in the  $(\epsilon, D)$  plane for the initial momentum distribution chosen as Waterbag (a) and Gaussian (b). The solid line is the thermodynamic phase boundary  $D(\epsilon_c)$  and the broken line is the dynamical boundary  $D(\epsilon^*)$ . The dotted line gives the line where  $\omega'$  vanishes. The dashed-dotted line is the first-order line where the magnetization changes its direction. Note that, in the Gaussian case, the dynamical and the thermodynamical boundaries coincide.

stable region  $\epsilon^* < \epsilon < \epsilon_c$  where long relaxation timescales increasing as a power of  $N$  are expected, an unstable regime  $\epsilon'^* < \epsilon < \epsilon^*$  with a single mode of instability namely  $\Omega$ , and another unstable regime  $\epsilon < \epsilon'^*$  with two modes of instability  $\Omega$  and  $\Omega'$  where  $\Omega^2 = -\omega^2$  and  $\Omega'^2 = -\omega'^2$ . Since  $\Omega > \Omega'$ , the magnetization increases exponentially fast with rate  $\Omega$ . Thus, in the last two regimes, the relaxation timescales diverging as  $\ln N$  are expected. The  $(\epsilon, D)$  phase diagram resulting from this analysis is given in figure 2(a).

Our numerical results for the time evolution of the magnetization in the unstable and the stable phases are shown in figure 3. For  $\epsilon < \epsilon^*$  (figure 3(a)), data collapse of the curves for various system sizes is observed when the magnetization is scaled with a factor  $\sqrt{N}$  as in the last section. Thus, we again obtain  $\ln N$  scaling for the relaxation time. The growth rate in the unstable phase is also in agreement with  $\omega$  in (33). For  $\epsilon > \epsilon^*$  (figure 3(b)), the magnetization stays close to its initial value  $\sim 1/\sqrt{N}$  for a long time which is consistent with  $N^{1.7}$  scaling as for the basic HMF model.

*Gaussian distribution.* For initial momentum chosen from Gaussian distribution, the dynamics are always unstable and the frequency  $\omega^2 = -\Omega^2$ ,  $\Omega$  real. Consider the integrals  $J_{\pm}$  defined in (16):

$$J_+ = J_- = \frac{\beta}{2} \left[ 1 - \Omega^2 \sqrt{\frac{\beta}{2\pi}} \int_{-\infty}^{\infty} dp \frac{e^{-\beta p^2/2}}{p^2 + \Omega^2} \right] \quad (35)$$

where we have used that the derivative of  $f^{(0)}$  is an odd function. The integral in the last term can be evaluated using the Schwinger trick:

$$\int_{-\infty}^{\infty} dp \frac{e^{-\beta p^2/2}}{p^2 + \Omega^2} = \int_{-\infty}^{\infty} dp e^{-\beta p^2/2} \int_0^{\infty} dq e^{-q(p^2 + \Omega^2)} = \frac{\pi}{\Omega} \exp\left(\frac{\beta\Omega^2}{2}\right) \text{Erfc}\left(\sqrt{\frac{\beta}{2}}\Omega\right). \quad (36)$$

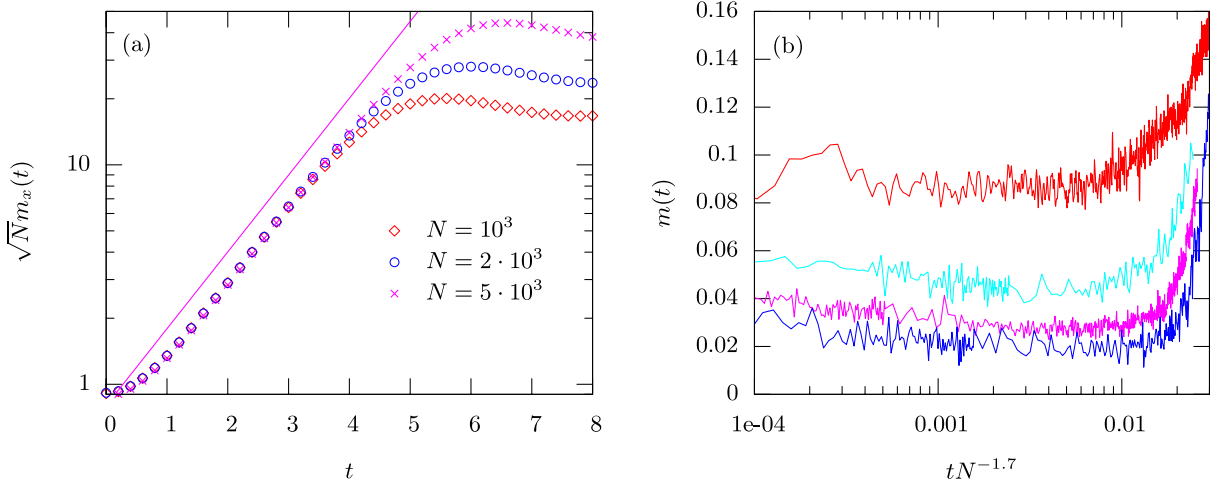


**Figure 3.** Temporal behavior of the magnetization in the anisotropic HMF model for uniformly distributed initial momentum. (a) The three curves in the unstable phase show scaled magnetization  $\sqrt{N}m_x(t)$  for  $\epsilon = 0.55$  and  $D = 0.9$ . The slope of the solid lines is given by  $\omega$  in (33). (b) Evolution in the stable phase with  $\epsilon = 0.8$  and  $D = 0.9$  (top to bottom) for  $N = 500(100)$ ,  $2000(50)$ ,  $5000(50)$ ,  $10000(5)$ . The number of histories over which data are averaged is given in parentheses. The scaled data is consistent with  $N^{1.7}$  scaling of the quasistationary lifetime.

Since the dispersion relation (31) is quadratic in  $J_+$  it has two solutions, namely  $J_+ = 1/(1 + D)$  and  $J_+ = 1$  with respective frequencies  $\Omega$  and  $\Omega'$  which obey

$$1 - \sqrt{\frac{\beta\pi}{2}}\Omega \exp\left(\frac{\beta\Omega^2}{2}\right) \text{Erfc}\left(\sqrt{\frac{\beta}{2}}\Omega\right) = \frac{2}{\beta(1 + D)} \quad (37)$$

$$1 - \sqrt{\frac{\beta\pi}{2}}\Omega' \exp\left(\frac{\beta\Omega'^2}{2}\right) \text{Erfc}\left(\sqrt{\frac{\beta}{2}}\Omega'\right) = \frac{2}{\beta}. \quad (38)$$

The real frequencies  $\Omega, \Omega'$  vanish at  $\epsilon^* = (3 + D)/4$  and  $\epsilon'^* = 3/4$ , respectively. The critical energy  $\epsilon^*( > \epsilon'^*)$  coincides with  $\epsilon_c$  as there is no stable phase when the initial momentum is distributed according to a Gaussian distribution. One is thus left with two unstable regimes, one with a single unstable mode ( $\epsilon'^* < \epsilon < \epsilon_c$ ) and the other with two unstable modes ( $\epsilon < \epsilon'^*$ ). Since the left-hand side of the above equations for  $\Omega$  and  $\Omega'$  is a monotonically decreasing function lying between 1 and 0, one has  $\Omega > \Omega'$  for  $D > 0$ . Thus we expect the growth rate of  $m_x$  to be  $\Omega$  for all energies below  $\epsilon_c$ . The dynamical phase diagram corresponding to the case of Gaussian initial distribution is given in figure 2(b). Our numerical results for the evolution of the magnetization verifying the conclusions presented above are shown in figure 4.

#### 4. Hamiltonian mean field model with on-site potential

We next consider the HMF model with cosine on-site potential whose Hamiltonian is

$$H = \frac{1}{2} \sum_{i=1}^N p_i^2 + \frac{1}{2N} \sum_{i,j=1}^N (1 - \cos(\theta_i - \theta_j)) + W \sum_{i=1}^N \cos^2 \theta_i. \quad (39)$$

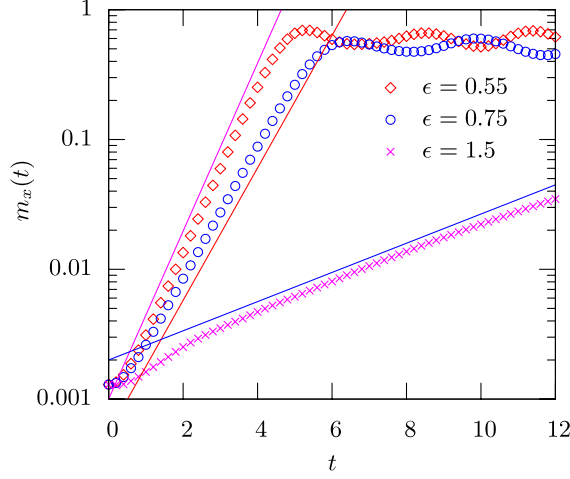


**Figure 4.** Semi-log plot of the magnetization as a function of time for Gaussian  $f^{(0)}(p)$  in the dynamically unstable, ferromagnetic phase for  $N = 5 \times 10^5$ ,  $D = 4$  and various  $\epsilon$ . The lines have a slope  $\Omega$  given by (37).

where the last term in the Hamiltonian gives the energy due to an on-site potential. For positive (negative)  $W$ , the steady state magnetization is along the  $y(x)$  axis and, in the following, we assume  $W > 0$ . The equilibrium properties of this model can be calculated following the same procedure outlined in section 2. The equilibrium magnetization  $\overline{m}_y$  along the  $y$  axis is determined by the following equation:

$$\overline{m}_y = \frac{\int_{-\pi}^{\pi} d\theta \sin \theta e^{\beta \overline{m}_y \sin \theta - \beta W \cos^2 \theta}}{\int_{-\pi}^{\pi} d\theta e^{\beta \overline{m}_y \sin \theta - \beta W \cos^2 \theta}}. \quad (40)$$

The magnetization vanishes at a critical temperature determined via  $\beta_c^{-1} = (I_0(z) + I_1(z))/2I_0(z)$  where  $I_0$  and  $I_1$  are the modified Bessel functions of the first kind and the argument  $z = \beta_c W/2$ . For positive  $W \ll 1$ , the critical temperature at which  $m$  becomes zero is given as  $(2 + W)/4$  to leading order in  $W$ . The critical energy  $\epsilon_c$  is then given by

$$\epsilon_c = \frac{1}{2\beta_c} + \frac{1}{2} + \frac{W}{\beta_c} \approx \frac{3}{4} + \frac{5W}{8}. \quad (41)$$

For the model defined by (39), the canonical equations of motion are

$$\frac{d\theta_i}{dt} = p_i, \quad \frac{dp_i}{dt} = -m_x \sin \theta_i + m_y \cos \theta_i + 2W \cos \theta_i \sin \theta_i. \quad (42)$$

As in the previous sections, for a large number of particles the dynamics is well approximated by the Vlasov equation (10) with the following potential:

$$V[f] = - \int_{p_{\min}}^{p_{\max}} dp' \int_{-\pi}^{\pi} d\theta' \cos(\theta - \theta') f(\theta', p', t) + W \cos^2 \theta. \quad (43)$$

Unlike for the models considered in the preceding sections, the homogeneous state is no longer a stationary state of the Vlasov equation due to the presence of the last term in the potential  $V$ . However, the distribution function  $f(\theta, p) = \Phi(e(\theta, p))$ , with arbitrary

function  $\Phi$ , where the single-particle energy  $e$  is given by

$$e(\theta, p) = \frac{p^2}{2} + V(\theta) = \frac{p^2}{2} - m_x \cos \theta - m_y \sin \theta + W \cos^2 \theta \quad (44)$$

are stationary solutions of the Vlasov equation (10). This can be easily seen by differentiating the Vlasov equation (10) and by noting that the potential energy  $V$  is a function of the angle variable only. We stress that the magnetization values  $m_x$  and  $m_y$  must be self-consistently determined. The particular case  $f^{(0)}(\theta, p) \sim \exp(-\beta e(\theta, p))$  is the statistical equilibrium density.

A special class of stationary distributions is given by  $f^{(0)}(\theta, p) = \Phi(p^2/2 + W \cos^2 \theta)$ . The fact that  $m_x = m_y = 0$  follows by symmetry arguments. In the following, we will study a waterbag stationary state distribution, i.e.  $\Phi$  is a step function

$$f^{(0)}(\theta, p) = \begin{cases} A, & \frac{p^2}{2} + W \cos^2 \theta < E \\ 0, & \text{otherwise.} \end{cases} \quad (45)$$

The distribution function  $f^{(0)}(p)$  is thus constant over the domain  $\mathcal{D}$  defined by

$$|p| < p_0(\theta) = \sqrt{2(E - W \cos^2 \theta)}, \quad (46)$$

and is simply connected for  $W < E$ . The study of the case  $W > E$  can be done following ideas similar to those described below. The normalization constant  $A$  is determined using  $\int_{-\pi}^{\pi} d\theta \int_{-p_0(\theta)}^{p_0(\theta)} dp f^{(0)}(\theta, p) = 1$  and we have

$$\frac{1}{2A} = \int_{-\pi}^{\pi} d\theta \sqrt{2(E - W \cos^2 \theta)}. \quad (47)$$

The parameter  $E$  can be related to the conserved initial energy  $\epsilon$  by performing the integration over the  $p$  variable in (39) and we obtain

$$\epsilon = A \int_0^{2\pi} d\theta \left\{ \frac{1}{3} [2(E - W \cos^2 \theta)]^{3/2} + 2W \cos^2 \theta [2(E - W \cos^2 \theta)]^{1/2} \right\}. \quad (48)$$

To compute the linear stability threshold, as before, we linearize the dynamics close to the stationary solution,  $f = f^{(0)} + \lambda f^{(1)} \exp(i\omega t)$ . The perturbation  $f^{(1)}$  then satisfies

$$i\omega f^{(1)} + p \frac{\partial f^{(1)}}{\partial \theta} - \frac{dV[f^{(0)}]}{d\theta} \frac{\partial f^{(1)}}{\partial p} - \frac{dV[f^{(1)}]}{d\theta} \frac{\partial f^{(0)}}{\partial p} = 0. \quad (49)$$

We will determine the energy  $\epsilon^*$  which corresponds to the neutral mode  $\omega = 0$ . Below this energy, the dynamics is expected to be unstable and stable above it. At  $\omega = 0$ , the above equation can be written explicitly as

$$p \frac{\partial f^{(1)}}{\partial \theta} - A [\delta(p + p_0(\theta)) - \delta(p - p_0(\theta))] \int dp' d\theta' \sin(\theta - \theta') f^{(1)}(\theta', p', \omega) + 2W \sin \theta \cos \theta \frac{\partial f^{(1)}}{\partial p} = 0. \quad (50)$$

We solve this last equation by a formal expansion in terms of Dirac distributions  $\delta$  and its order  $n$  derivatives  $\delta^{(n)}$ :

$$f^{(1)} = \sum_{n=0}^{\infty} a_n(\theta) \delta^{(n)}(p + p_0(\theta)) + b_n(\theta) \delta^{(n)}(p - p_0(\theta)). \quad (51)$$

The equations for  $a_n$  and  $b_n$  and their solutions can be found recursively. We report the analysis only for  $a_0$  and  $b_0$ :

$$\frac{da_0}{d\theta} = \frac{db_0}{d\theta} = A \frac{\sin \theta m_x[\delta f] - \cos \theta m_y[\delta f]}{p_0(\theta)}. \quad (52)$$

The magnetization  $m_x[\delta f]$  must be determined self-consistently from the distribution function. Using (51), the formula (52) and (47), we obtain

$$\int_{-\pi}^{\pi} d\theta \sqrt{2(E - W \cos^2 \theta)} = \int_{-\pi}^{\pi} d\theta \frac{\sin^2 \theta}{\sqrt{2(E - W \cos^2 \theta)}}. \quad (53)$$

This is the equation for the marginal stability of the inhomogeneous waterbag distribution function. We define

$$I(x) = \frac{1}{\int_0^{2\pi} d\theta \sqrt{1 - x \cos^2 \theta}} \int_0^{2\pi} d\theta \frac{\sin^2 \theta}{\sqrt{1 - x \cos^2 \theta}} \quad (54)$$

which can be expressed in terms of complete elliptic functions of the first and second type. The equation for the marginal stability for inhomogeneous waterbag distributions is then

$$2E = I\left(\frac{W}{E}\right). \quad (55)$$

One can prove that  $I$  is a strictly decreasing function from the interval  $[0; 1]$  onto the interval  $[1/2; 1]$ .  $I^{-1}$  is thus an increasing function from  $[1/2; 1]$  onto  $[0; 1]$ . From this, one can prove that the equation  $I^{-1}(2E) = W/E$  has a single solution  $E^*(W)$  for each value of  $W$  in the range  $[0; 1/2]$ , and no solutions for  $W > 1/2$ . For  $W = 1/2$ , we have  $E^* = W$ ; this is the limit above which the inhomogeneous waterbag ceases to be simply connected (see the discussion below (46)). For values larger than  $W = 1/2$ , the transition value  $E^*(W)$  could be studied by considering doubly connected domains.

For  $W \ll 1$ , equation (53) can be easily linearized and we obtain  $E^*(W) = 1/4 + 3W/8 + O(W^2)$ . Now using (48), we can compute the critical  $\epsilon^*(W)$  as a function of  $W$ . For instance, for  $W \ll 1$ , we obtain

$$\epsilon^*(W) = \frac{7}{12} + \frac{11W}{24} + O(W^2). \quad (56)$$

For  $W = 0$ , we obtain the critical energy for the homogeneous waterbag distribution  $\epsilon^* = 7/12$  (see [16]). For any value  $0 \leq W \leq 1/2$ , the critical value of the energy can easily be computed numerically from (55). Figure 5 shows the curve of marginal stability.

At energies below  $\epsilon^*(W)$ , where the waterbag state is unstable, the relaxation time grows logarithmically with the system size, as in the case of the model with global anisotropy. This is a result of the fact that the initial magnetization of the waterbag state is of the order of  $1/\sqrt{N}$ . For energies above  $\epsilon^*(W)$  where the waterbag state is linearly stable, we expect a longer relaxation time, which grows algebraically with  $N$ .

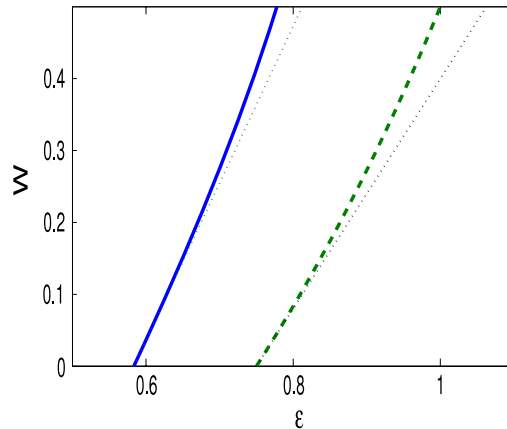


**Figure 5.** Dynamical phase diagram in the  $(\epsilon, W)$  plane for the inhomogeneous uniform distribution of the HMF model with on-site potential. The bold line is the line of marginal stability  $W(\epsilon^*)$  and the thermodynamic phase boundary  $W(\epsilon_c)$  is shown as a dashed line. The dotted lines are the respective curves obtained within the linear approximation for  $W \ll 1$  given in (41) and (56).

## 5. How long is the Vlasov approximation valid?

In this section, we discuss the validity of the approximation of the  $N$ -particle phase-space distribution

$$f_d(\theta, p, t) = \frac{1}{N} \sum_{i=1}^N \delta(\theta_i(t) - \theta) \delta(p_i(t) - p) \quad (57)$$

by a smooth density function  $f_s(\theta, p, t)$ , where both  $f_d$  and  $f_s$  satisfy the Vlasov equation (10) (mean field approximation). We ask: how long is this approximation justified?

We consider an ensemble of initial conditions for the  $N$  particles  $\{(\theta_i(t=0), p_i(t=0))\}_{1 \leq i \leq N}$ . We suppose that the corresponding  $f_d(t=0)$  is close to some smooth distribution function  $f_s(t=0)$  (i.e. the distance between  $f_d$  and  $f_s$  converges to zero as  $N$  goes to infinity). If for almost all initial conditions,  $f_d$  remains close to the smooth  $f_s$ , we say that the system has a kinetic behavior: all trajectories remain close to each other. The kinetic evolution is then the solution of the Vlasov equation with initial condition  $f_s(t=0)$ . The issue of the validity of the mean field approximation, or equivalently of the validity of the kinetic description, is to know for how long all trajectories remain close to  $f_s$ . Since  $f_d$  satisfies the Vlasov equation, this issue is related to the stability of the Vlasov equation.

Let us first summarize the known results. The validity of this mean field approximation for large  $N$  has been established mathematically, for smooth potential  $V$ , by Braun and Hepp [46] (see also [49]). More precisely, the theorem of Braun and Hepp states that, for a mean-field microscopic two-body smooth potential, the distance between two initially close solutions of the Vlasov equation increases at most exponentially in time. Indeed, if  $f(t)$  and  $g(t)$  are two solutions, if  $\Delta(f, g)(t=0)$  is sufficiently small, then  $\Delta(f, g)(t) \leq \Delta(f, g)(0) \exp(at)$ , where  $\Delta$  is the Wasserstein distance and  $a$  is a constant.

This result can be applied to the approximation of the  $N$ -particle Hamiltonian dynamics by the Vlasov equation. We consider, for the  $N$ -particle dynamics, an ensemble of initial conditions  $\{(\theta_i, p_i)_{1 \leq i \leq N}\}$  distributed according to the measure  $f(\theta_1, p_1, \dots, \theta_N, p_N) = \prod_{i=1}^N f_s(\theta_i, p_i)$ . For large  $N$ , for a typical initial condition, the phase-space initial distribution  $f_d(\theta, p, 0)$  will be close to  $f_s(\theta, p, 0)$ . Typically  $\Delta(f_d, f_s)(t=0) = \mathcal{O}(1/N^\alpha)$  with  $\alpha > 0$ . Let us consider  $f_s$  the solution of the Vlasov equation with initial condition  $f^{(0)}$ . Because  $f_d$  and  $f_s$  are both solutions for the Vlasov equation, we can apply the Braun and Hepp result. If we define  $t_V$  to be the time at which the error  $\Delta(f_d, f_s)$  is of order unity, the theorem then implies that  $t_V$  increases at least as  $\ln N$  when  $N \rightarrow \infty$  (for this argument, see also [16]).

In sections 2 and 3, we have considered the special case where the initial distribution  $f^{(0)}$  is a stationary solution of the Vlasov equation. When  $f^{(0)}$  is unstable, the perturbation  $f^{(1)}$  grows exponentially. We have explained and illustrated that  $t_V$  is proportional to  $\ln N$ . Thus the trajectories diverge from  $f_s$  on a timescale given by  $\ln N/\Omega$ . This thus proves that the Braun and Hepp result for  $t_V$  is not only a lower bound, but is actually achieved. After this timescale, the trajectories diverge and the system does not have a kinetic behavior any more.

When  $f^{(0)}$  is a *stable* stationary solution of the Vlasov equation,  $t_V$  is the stability time of the quasi-stationary state. A very recent work [47] has proven that the  $N$ -particle dynamics actually remains close to the stationary solutions, at least for times of the order of  $N^{1/8}$ , when the potential  $V$  is sufficiently smooth. On physical grounds, using kinetic theory, one expects the validity time to be of the order of  $N$  for systems in which each particle is characterized by more than one dynamical variable. When no resonance between trajectories is possible, as is the case for systems with one dynamical variable, one expects validity times to be much larger than  $N$  [23]. This peculiarity of  $1d$  systems has been numerically observed in the HMF model, where times of the order of  $N^{1.7}$  have been measured for homogeneous quasi-stationary states [16]. This timescale seems to be robust with respect to the perturbations of the Hamiltonian as we have demonstrated for the anisotropic case in section 3.

Let us now consider the more general case when the initial condition is close to a distribution  $f$  which is not stationary. In accordance with the observed phenomenology for the Vlasov equation, one expects that  $f$  will have a rapid relaxation in a finite time either towards a quasi-stationary state, or towards a periodic solution, or towards a statistical equilibrium for the Vlasov equation. Because this first stage takes place in times which are of order one (which do not depend on  $N$ ), one expects that this initial relaxation will have a negligible effect on the long time error. The validity time for the Vlasov approximation will then be given by the validity time of the quasi-stationary states. Then times  $t_V$  of the order of  $N^\alpha$  are expected. We thus conjecture that, for generic initial distributions, the approximation by the Vlasov equation is valid over times which are the lifetime for the quasi-stationary states.

## 6. Conclusions

In this paper, we studied the short time dynamics of models with long ranged Hamiltonians. In each case, starting from the initial magnetization of the order of  $1/\sqrt{N}$ , the time required to achieve a finite value of  $m$  scales with the number  $N$  of particles.

This behavior is different from that of the corresponding short ranged Hamiltonians where such time is of order unity. The dynamics were studied by a numerical integration of the Hamilton's equations of motion and a stability analysis of the Vlasov equation. The latter analysis shows that, close to the unstable stationary states of the Vlasov equation, the relaxation occurs over a time  $\sim \ln N$  while close to stable stationary states, the system stays in a quasistationary state whose lifetime goes as a power law in  $N$ .

So far we considered only the deterministic dynamics. An interesting direction would be to study such models when the dynamical rules are stochastic. One such case has been discussed in [13] where the system of Ising spins evolves via microcanonical Monte Carlo dynamics. Since the Ising energy can be obtained as a limiting case of the Hamiltonians considered here (with anisotropy or on-site potential), it would be worthwhile to study these systems with stochastic evolution rules. Besides, for the HMF model, the ensemble equivalence in the equilibrium steady state has been shown using the large deviation method [48]. Recent numerical studies [38, 52] of the dynamics of this system in contact with a thermal bath have focused on the stable regime  $\epsilon > \epsilon^*$  and find that the quasistationary states seen in the microcanonical ensemble survive but the lifetime increases as a power law (in  $N$ ) with an exponent that decreases with increasing system–bath coupling. It would be interesting to know if the unstable phase exhibits a similar dependence on the coupling with the heat reservoir.

## Acknowledgments

Financial support of the Israel Science Foundation (ISF) is acknowledged. The visit of FB to the Weizmann Institute has been supported by the Albert Einstein Minerva Center for Theoretical Physics.

## References

- [1] Dauxois T, Ruffo S, Arimondo E and Wilkens M (ed), 2002 *Dynamics and Thermodynamics of Systems with Long Range Interactions (Lecture Notes in Physics vol 602)* (Berlin: Springer)
- [2] Lynden-Bell D and Wood R, 1968 *Mon. Not. R. Astron. Soc.* **138** 495
- [3] Hertel P and Thirring W, 1971 *Ann. Phys.* **63** 520
- [4] Smith R A and O'Neil T M, 1990 *Phys. Fluids B* **2** 2961
- [5] Caglioti E, Lions P L, Marchioro C and Pulvirenti M, 1990 *Commun. Math. Phys.* **174** 229
- [6] Kiessling M K H and Neukirch T, 2003 *Proc. Nat. Acad. Sci.* **100** 1510
- [7] Miller B N and Youngkins P, 1998 *Phys. Rev. Lett.* **81** 4794
- [8] Chavanis P H and Ispolatov I, 2002 *Phys. Rev. E* **66** 036109
- [9] Ellis R S, Haven K and Turkington B, 2002 *Nonlinearity* **15** 239
- [10] Antoni M, Ruffo S and Torcini A, 2002 *Phys. Rev. E* **66** 025103
- [11] Dauxois T, Lepri S and Ruffo S, 2003 *Commun. Nonlinear Sci. Numer. Simul.* **8** 375
- [12] Barré J, Mukamel D and Ruffo S, 2001 *Phys. Rev. Lett.* **87** 030601
- [13] Mukamel D, Ruffo S and Schreiber N, 2005 *Phys. Rev. Lett.* **95** 240604
- [14] Bouchet F and Barré J, 2005 *J. Stat. Phys.* **118** 1073
- [15] Latora V, Rapisarda A and Ruffo S, 1998 *Phys. Rev. Lett.* **80** 692
- [16] Yamaguchi Y Y, Barré J, Bouchet F, Dauxois T and Ruffo S, 2004 *Physica A* **337** 36
- [17] Dubin D H E and O'Neil T M, 1999 *Rev. Mod. Phys.* **71** 1
- [18] Spitzer L, 1987 *Dynamical Evolution of Globular Clusters (Princeton Series in Astrophysics)* (Princeton, NJ: Princeton University Press)
- [19] Firpo M C, 1998 *Phys. Rev. E* **57** 6599
- [20] Latora V, Rapisarda A and Ruffo S, 1999 *Phys. Rev. Lett.* **83** 2104
- [21] Yamaguchi Y Y, 2003 *Phys. Rev. E* **68** 066210
- [22] Pluchino A, Latora V and Rapisarda A, 2004 *Phys. Rev. E* **69** 056113
- [23] Bouchet F and Dauxois T, 2005 *Phys. Rev. E* **72** 045103

- [24] Yamaguchi Y, Bouchet F and Dauxois T, 2007 *J. Stat. Mech.* [P01020](#)
- [25] Borgonovi F, Celardo G L, Maianti M and Pedersoli E, 2004 *J. Stat. Phys.* **116** 1435
- [26] Del-Castillo-Negrete D, 2000 *Physica A* **280** 10
- [27] Nicholson D R, 1983 *Introduction to Plasma Theory* (New York: Wiley)
- [28] Dubin D H E, 2003 *Phys. Plasmas* **10** 1338
- [29] Chavanis P H, 2000 *Phys. Rev. Lett.* **84** 5512
- [30] Bray A J, 1994 *Adv. Phys.* **43** 357
- [31] Bouchet F and Dauxois T, 2005 *J. Phys.: Conf. Ser.* **7** 34
- [32] Latora V, Rapisarda A and Tsallis C, 2001 *Phys. Rev. E* **64** 056134
- [33] Pluchino A, Latora V and Rapisarda A, 2004 *Physica A* **340** 187
- [34] Barré J, Dauxois T, De Ninno G, Fanelli D and Ruffo S, 2004 *Phys. Rev. E* **69** 045501(R)
- [35] Antoniazzi A, Fanelli D, Barre J, Dauxois T, Chavanis P H and Ruffo S, 2006 *Phys. Rev. E* **75** 011112
- [36] Chavanis P H, 2006 *Eur. Phys. J. B* **53** 487
- [37] Campa A, Giansanti A, Mukamel D and Ruffo S, 2006 *Physica A* **365** 120
- [38] Baldovin F and Orlandini E, 2006 *Phys. Rev. Lett.* **96** 240602
- [39] Baldovin F and Orlandini E, 2006 *Phys. Rev. Lett.* **97** 100601
- [40] Antoni M and Ruffo S, 1995 *Phys. Rev. E* **52** 2361
- [41] Zaslavsky G M, Shabanov V F, Aleksandrov K S and Aleksandrov I P, 1977 *Sov. Phys. JETP* **45** 315
- [42] Konishi T and Kaneko K, 1992 *J. Phys. A* **25** 6283
- [43] del-Castillo-Negrete D, 2002 *Dynamics and Thermodynamics of Systems with Long Range Interactions* (*Springer Lecture Notes in Physics* vol 602) ed T Dauxois, S Ruffo, E Arimondo and M Wilkens (Berlin: Springer)
- [44] Pichon C, 1994 *PhD Thesis* Cambridge
- [45] Inagaki S and Konishi T, 1993 *Publ. Astron. Soc. Japan* **45** 733
- [46] Braun W and Hepp K, 1977 *Commun. Math. Phys.* **56** 101
- [47] Caglioti E and Rousset F, 2007 *Commun. Math. Sci.* **5** 11
- [48] Barré J, Bouchet F, Dauxois T and Ruffo S, 2005 *J. Stat. Phys.* **119** 677
- [49] Spohn H, 1991 *Large Scale Dynamics of Interacting Particles* (New York: Springer)
- [50] Firpo M C and Elskens Y, 1998 *J. Stat. Phys.* **93** 193
- [51] Elskens Y and Escande D F, 2002 *Microscopic Dynamics of Plasmas and Chaos* (Bristol: Institute of Physics Publishing)
- [52] Morita H and Kaneko K, 2004 *Europhys. Lett.* **66** 198